Department of Physics and Astronomy
University of Heidelberg

Bachelor Thesis in Physics
submitted by

Marius Blaesing

born in Villingen-Schwenningen (Germany)

2013

Methods for explaining quantum dynamics of Kicked Atoms

2

This Bachelor Thesis has been carried out by Marius Blaesing at the
Institute of Theoretical Physics in Heidelberg
under the supervision of
PD Dr. Sandro Wimberger

Contents

Abstract

This thesis examines methods to explain quantum dynamics of atoms in a time- and space-periodic kicking potential in the context of a recent and novel experimental realisation of the unfolded Quantum Kicked Rotor at the Friedrich-Alexander-Universität Erlangen. In order to understand the diffusive behaviour of the wave-package for a larger parameter range, Husimi-mappings of the quantum states are used. These allow after examination of analogies between both models to explain properties of the Quantum Kicked Rotor through trajectories in the phasespace of its classical counterpart. Moreover, characteristic quantum transport patterns of the unfolded model in position-space can be traced back to a phasespace-mapping of the original Quantum Kicked Rotor's time evolution.

Zusammenfassung

Die Arbeit untersucht Methoden zur Erklärung der Quantendynamik von Atomen in einem Zeit- und Ort-periodischen Kick-Potential im Kontext einer neuartigen experimentellen Realisation des entfalteten Quantum Kicked Rotors an der Friedrich-Alexander-Universität Erlangen aus der jüngeren Vergangenheit. Um das Diffusionsverhalten der Wellenfunktion für einen größeren Parameter-Bereich verstehen zu können, werden Husimi-Abbildungen der Quanten-Zustände gebildet. Diese ermöglichen es nach Beobachtung von Analogien der beiden Modelle Eigenschaften des quantenmechanischen Kicked Rotors durch Trajektorien im Phasenraum seines klassischen Pendants zu erklären. Zudem können charakteristische Quanten Transport-Muster des entfalteten Modells im Ortsraum auf eine Phasenraumabbildung der Zeitentwicklung des originalen Quantum Kicked Rotors zurückgeführt werden.

1. Introduction and Outline

After a new optical experiment of the well-studied Quantum Kicked Rotor had been realized at the Friedrich-Alexander University of Erlangen, theoretical research was re-initialized on the topic. This thesis develops the theory in position-space of atoms being kicked by an external periodic driving force further. The initial issue of theoretical research is the diffusion of wave-packages in position-space, coming from an unfolded Quantum Kicked Rotor. These represent ultra-cold atoms, which where examined in earlier Quantum Kicked Rotor experiments. Why do they show varying diffusion behaviour for changing parameters of the system, e.g. kicking-strength and time period between two kicks? The main goal of this topic is to explain this behaviour for a broader parameter range, as an analytical theory could only be found for a small range of kicking strengths k.

This will be achieved by connecting the experimental realisation of Kicked Atoms to the theoretical model of the Kicked Rotor via Bloch's theorem in chapter 2: The experiment's position-space is put into relation to the angular momentum-space of a Kicked Rotor. On this level of abstraction, one can relate the classical and quantum mechanical versions of the Kicked Rotor model. The time evolutions of both models can be simulated easily numerically. It is possible to get hints on possible relations between the models. In some cases it is possible to deduce information from the classical model explaining the quantum mechanical behaviour.
The links between the classical and quantum mechanical realisations are relations of their variables/observables, a projection of quantum states to the classical phase space using Husimi-functions or the action angle-formulation of the classical Kicked Rotor problem, which links to a quantum mechanical quantisation law.

In chapter 3, the results of the introduced measures will be discussed and combined to develop the theory of Kicked Atoms further. Relations of quantum and classical mechanics will be checked with respect to Kicked Rotors. It will be shown, that both approaches to the problem show comparable behaviour for specific setups or parameter ranges. These analogies are mainly examined by introduction of e.g. chaotic-trajectories related custom observables which allow a comparison of the system. Furthermore, Husimi-mappings are used to either support or decline these analogies.

Chapter 4 summarizes the results and gives a possible outlook of further studies.

2. Theory

2.1. Connecting the Experiment, the Quantum Kicked Rotor and the Standard Map

This thesis continues the examinations of the Atom Optics Kicked Rotor which is described by the Kicked Rotor model and was started by an experiment by Raizen [5] and theoretically examined in [2],[12] and [10]. Based on further results in [14] some new relations between the known and examined models are introduced.

2.1.1. Modelling laser-kicked atoms: Relation of the Experiment and the Quantum Kicked Rotor

The Quantum Kicked Rotor can be used to model the time evolution of laser-kicked atoms in a sinusoidal potential as sketched in Figure 2.1. The corresponding experiment yields data of the wave-function in position-representation $\psi(x,t)$. Since this wave-function describes a quantum-state within a peroidic potential, Bloch's theorem can be used to factorize it into a periodic and a phase part. It is possible to describe the state in position-space as a superposition of Quantum Kicked Rotors residing in angle-space. Each of these Quantum Kicked Rotors has quasi-momentum β [6], which is a constant of the motion:

$$\psi(x,t) = \int\limits_0^1 \rho(\beta)e^{i\beta x}\psi_\beta(x = \theta, t)d\beta \tag{2.1}$$
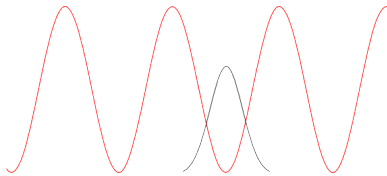

Figure 2.1.: Visualisation of an initial quantum state (black) in sinusoidal potential (red) resulting from a standing wave of a laser-pulse.

Since the actual angular momentum n needs to be of integer-type on the rotor (quantization of angular momentum), it splits into $p = n + \beta$, where β again represents the quasi-momentum associated with each so-called β-rotor.

The relation derived in (2.1) can be used to obtain a wave-function in position-space from the β-rotor in angle-space. Each of the underlying rotors, a Quantum Kicked Rotor, can be simulated easily. An inverse Fourier-Transform of the Quantum Kicked Rotor's representation in angle-space yields its wave-function in angular momentum-representation in which the initial state will be defined:

$$\mathcal{F}^{-1}(\psi_\beta(\theta, t))(p, t) = \int\limits_{-\pi}^{\pi} e^{ip\theta}\psi_\beta(\theta, t)d\theta = \psi(p, t) \tag{2.2}$$

The initial state in angular momentum-representation can be defined as coherent state and thus

$$\sigma_n \cdot \sigma_\theta = \frac{1}{2} \tag{2.3}$$

holds. It then satifies Heisenberg's uncertainty relation $\Delta x \Delta p \geq \frac{1}{2}$, where $\hbar$ was set to 1 because the dimensionless units introduced in the next section were already used. The Gaussian defined below fulfils the condition in (2.3) and will be used for further simulations. The explicit definition of this coherent state is (based on general findings [6] and adoptions to the discrete case [14]:

$$\psi_c(n, t = 0) = \frac{1}{\sqrt{\sqrt{2\pi}\sigma_n}} exp\left(-\frac{(n - n_0)^2}{4\sigma_n^2} - in\theta_0\right) \tag{2.4}$$

2.1.2. Relation of the Quantum Kicked Rotor and the Standard Map

The underlying Hamiltonian for the experimental realisation of the problem is motivated as ultra-cold atoms being driven by an external laser-pulse which is periodic in time (delta-kicks) and position (sinusoidal) as it is visualized in Figure 2.1.

The Hamiltonian describing this system is:

$$H' = \frac{p'^2}{2m} + V_0 \cos(2\pi\frac{x}{a}) \sum_{j=-\infty}^{\infty} \delta(t - j\tau') \tag{2.5}$$

7

This Hamiltonian is rescaled and transformed to dimensionless form H by dividing by $8E$ with $E = \frac{\hbar^2 k^2}{2m} = \frac{p^2}{2m}$ and $p = \hbar k$, e.g. making use of the lattice-periodicity of the problem [1], where $k = \frac{\pi}{a}$:

$$H = \frac{H'}{8E} = \frac{p'^2}{2m} \cdot \frac{2m}{8k^2\hbar^2} + \frac{2m}{8k^2\hbar^2} \cdot V_0 \cos(2\pi\frac{x}{a}) \sum_{j=-\infty}^{\infty} \delta(t - j\tau') \tag{2.6}$$

Setting (making use of an arbitrary scaling-constant T of dimension $[s^1]$, the effective experimental pulse length/duration [12])

$$p(p') = \frac{p'}{2\hbar k} \tag{2.7}$$

$$\tau(\tau') = \frac{8ET}{\hbar}\tau' \tag{2.8}$$

$$E = \frac{\hbar^2 k^2}{2m} \tag{2.9}$$

$$k(V_0) = \frac{V_0 T}{\hbar} \tag{2.10}$$

$$\theta(x) = 2kx \mod 2\pi \tag{2.11}$$

yields

$$H(p, \theta, t) = \frac{p^2}{2}\tau - k\cos(\theta) \sum_{j=-\infty}^{\infty} \delta(t - j\tau) \tag{2.12}$$

Introducing the new variables also shows the relation of $\hbar$ and τ:

$$\tau(\tau') = \frac{8ET}{\hbar}\tau' \propto \frac{\hbar^2}{\hbar} \tag{2.13}$$

$$\tau \propto \hbar \tag{2.14}$$

Finally, both the Quantum and the classical Kicked Rotor are described by the same time-dependent Hamiltonian (with the angular-momentum p and the angle θ being replaced by the respective operators in the quantum mechanical case):

$$H(p, \theta, t) = \frac{p^2}{2}\tau - k\cos(\theta) \sum_{j=-\infty}^{\infty} \delta(t - j\tau) \tag{2.15}$$

This yields the following iterative equations of motion for the classical version, obtained by integration over one time period of duration τ

$$p_{t+1} = p_t + K \sin(\theta_t) \tag{2.16}$$

$$\theta_{t+1} = \theta_t + p_{t+1}, \tag{2.17}$$

where $K = k\tau$ holds.

The quantum mechanical time evolution operator U is derived by integrating as usual, again over one time period of duration τ [9]:

$$\hat{U} = exp(-i \int_t^{t+\tau} H(t)dt) \tag{2.18}$$

$$= e^{-ik\cos(\hat{\theta})} e^{-i\tau \frac{\hat{p}^2}{2}} \tag{2.19}$$

$$=: \hat{K}\hat{F} \tag{2.20}$$

where $\hbar$ is set to 1 in (2.18) using the dimensionless units defined above. At this point, the operators representing kicking $\hat{K}$ and free evolution $\hat{F}$ were introduced. Notably $\hat{K}$ is diagonal in angle-representation, $\hat{F}$ is diagonal in angular momentum-representation.

Now, one can derive relations between classical variables and quantum mechanical observables [13]. Beginning from the Hamiltonian describing both cases, one can also introduce the splitting $p = n + \beta$ in classical mechanics by perceiving β as a scalar momentum-offset without further meaning.

$$H(t') = \frac{(n+\beta)^2}{2} + k\cos(\theta) \sum_t (t' - t\tau) \tag{2.21}$$

$$= \frac{n^2}{2} + n\beta + \frac{\beta^2}{2} + k\cos(\theta) \sum_t (t' - t\tau) \tag{2.22}$$

One then can derive the classical Hamiltonian equations of motion.

$$\dot{n} = -\frac{\partial H}{\partial \theta} = +k\sin(\theta) \tag{2.23}$$

$$\dot{\theta} = \frac{\partial H}{\partial n} = n + \beta \tag{2.24}$$

An interative expression incorporating the evaluation of n and θ only in time-intervalls τ is:

$$n_{t+1} = n_t + \int_0^\tau \dot{n}dt' = n_t + k\sin(\theta_t) \tag{2.25}$$

$$\theta_{t+1} = \theta_t + \int_0^\tau \dot{\theta}dt' = \theta_t + (n_{t+1} + \beta)\tau = \theta_t + n_{t+1}\tau + \beta\tau \tag{2.26}$$

Transforming $n \to \frac{n'}{\tau}$ yields:

$$n_{t+1} = n_t + k\tau\sin(\theta_t) \tag{2.27}$$

$$\theta_{t+1} = \theta_t + n_{t+1} + \tau\beta \tag{2.28}$$

Comparing the above result to the usual classical standard map

$$p_{t+1} = p_t + k\tau\sin(\theta_t) \tag{2.29}$$

$$\theta_{t+1} = \theta_t + p_{t+1} \tag{2.30}$$

yields the following relation between classical and quantum mechanical momenta:

$$p_{cl.} = n + \tau\beta = \tau p_{qm.} \tag{2.31}$$

$$\theta_{cl.} = \theta_{qm.} \tag{2.32}$$

Now use (2.3)

$$\sigma_{n_{cl.}} = \tau\sigma_{n_{qm.}} \tag{2.33}$$

$$\sigma_{\theta_{cl.}} = \sigma_{\theta_{qm.}} \overset{(2.3)}{=} \frac{1}{2\sigma_{n_{qm.}}} \tag{2.34}$$

to obtain a relation between the classical variables and quantum mechanical observables. By these relations one can get a first impression whether a quantum state resides rather in corresponding chaotic or regular phase space.
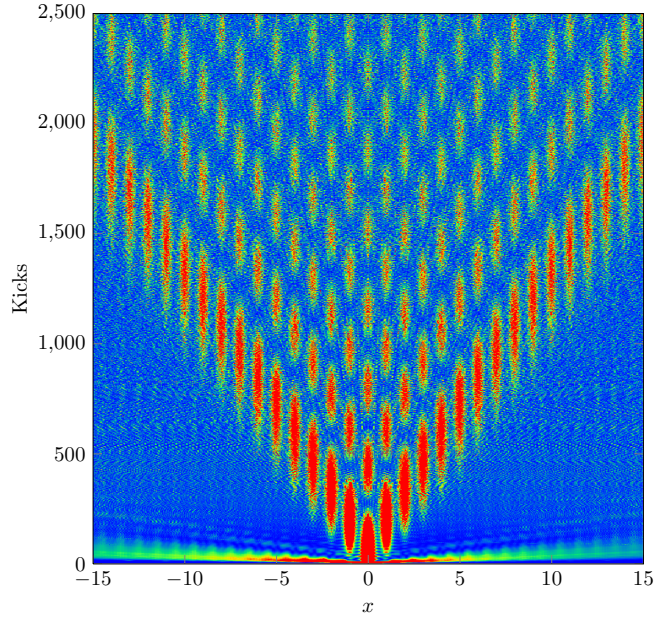
Figure 2.2.: Simulated data of the time evolution of $\psi(x,t)$. Red: Areas of higher probability-density, Blue: Areas of lower probability-density. For the used parameter set $k = 0.24, \tau = 0.66$ an analytical tunelling theory incorporating a next-neighbor-approximation/tight-binding-approximation which describes the diffusion velocity can be found.

2.2. Survival Probability of the Standard Map

When observing the time-evolution of the initial state in position-space for varying parameters k, τ, one can clearly notice a k-dependent diffusion tendency (of leaving the initial $[0, 2\pi] \times [0, 2\pi]$-cell). As discovered in [14], an analytical model can be found for the parameter range $k = [0.24, 0.44], \tau = 0.66$. It is one goal of this thesis to extend this range further.

The so-called Survival Probality is used to measure diffusion and characterize its time-dependent behaviour. In Figure 3.3.2, the diffusion over time of the initial wave can be clearly seen. In this case, it occurs to be of constant diffusion velocity $v = \frac{\Delta x}{\Delta t}$, which was adressed in [14] analytically.

However, measuring the diffusion velocity is not suitable for all parameter ranges of k, τ. As a more simple measure, the Survival Probability is introduced in [14]: The probability for a coherent initial state in position-space to stay in the initial zone of width 2π is then defined as

$$P_{Surv}(t) := \int\limits_{-\pi}^{\pi} |\psi(x,t)|^2 dx \tag{2.35}$$

As a classical counterpart, one can introduce a classical decay rate, which will be done ad-hoc during the presentation of the results of this thesis.

2.3. Action-angle Coordinates: Application to approximate Action of Tori

In order to discuss the diffusion-process of a state driven by an external time- and position-periodic potential, it is possible to compare the quantum mechanical system with the classical phasespace resulting from the classical Kicked Rotor.

Action-angle coordinates (I, Θ) allow one measuring the area or action of the central island of the classical Kicked Rotor easily. Trajectories within the regular island do not leave it, trajectories approaching it from the outside get repelled. This set of coordinates is introduced by the usual definition [8]

$$p = -\sqrt{2I}\sin(\Theta) \tag{2.36}$$

$$\theta = \sqrt{2I}\cos(\Theta) \tag{2.37}$$

Solving for the new pair of variables (I, Θ) yields:

$$I(\theta, p) = \frac{1}{\gamma}\left(\frac{p^2}{2} + \gamma^2\frac{\theta^2}{2}\right) \tag{2.38}$$

$$\Theta(\theta, p) = \tan^{-1}\left(\frac{p}{\gamma^2\theta}\right) \tag{2.39}$$

γ represents a squeezing-factor for the ellipsis-like Standard Map tori. Varying it, one can transform this ellipsis to a circle-like shape. The action of a certain torus can then be measured by integration of $I(\Theta)$. The measured action in combination with a action-quantisation law for states can tell how many quantum states live on the central island.

2.4. Analysis of the Quantum Kicked Rotor's Eigenstates

In order to analyse the time evolution of the Quantum Kicked Rotor, one needs to find the eigenstates and -values of the corresponding operator might give valuable hints.

In order to obtain these, it is necessary to diagonalize the time evolution operator $\hat{U}$. This will be done in angular momentum-representation. Since $\hat{K}$ operates in angle-space, it is necessary to perform a Fourier-Transform on it [12] to obtain the matrix elements of $\hat{U} = \hat{K}\hat{F}$ in angular momentum-representation [4]:

$$\langle n | \hat{U} | m \rangle = e^{-i\tau \frac{m^2}{2}} (-i)^{(n-m)} J_{(n-m)}(k) \tag{2.40}$$

where $J_i(k)$ is the Bessel-function of the First Kind of order i.

Now, one can obtain eigenvalues and eigenstates of the time evolution operator $\hat{U}$:

$$\hat{U} | \phi_j \rangle = e^{i\phi_j} | \phi_j \rangle \tag{2.41}$$

$$\{ | \phi_j \rangle \}_j \tag{2.42}$$

So far no eigenstate is of a particular meaning for further observation. By introducing the overlap of the eigenstates of $\hat{U}$ and the initial Gaussian-state $\psi_c(n, t)$ (residing in the center of the corresponding classical phase space: $n_0 = 0$ and $\theta_0 = 0$), this can be changed:

$$\| \langle \psi_c | \phi \rangle \|^2 (\phi) \tag{2.43}$$

Now, the set of eigenstates can be ranked by their overlap with the initial coherent state as described in (2.4). The state with the largest similarity can be considered as the one residing on the central island of the corresponding phase space. A large enough central island exists in the (conservatively sized) intervall $k\tau \in [0.2, 4]$.

2.5. Transformation to Classical Phasespace using Husimi-Functions

In order to discover the relation between the Quantum and Classical Kicked Rotor further, it is possible to project a quantum state $| \psi \rangle$ onto phase space via (the mapping is known as Husimi function [3]):

$$Q_{| \psi \rangle}(\theta_0, p_0) := \frac{1}{\pi} \| \langle \psi_c(\theta_0, p_0) | \phi \rangle \|^2 \tag{2.44}$$

This allows us to get hints on whether a quantum state resides in a region of classical chaos, which can indicate a classical diffusion process, or not. Furthermore, it might also be possible to validate the amount of stable states determined by using action-angle coordinates. One can also determine, whether the states distinguished by (2.43) really are the ones residing on the central island. Moreover, the time evolution of the Quantum Kicked Rotor can be made visible.

The Husimi-quasiprobability function was chosen among other quasiprobability functions such as the Wigner function, because it does not violate Heisenberg's uncertainty principle: "It does not serve as a probability density for finding a particle at a point in phase space, but as a probability density for observing the particle in a minimum uncertainty state" such as the introduced Gaussian (2.4) centered at a specified phase space point [3].

3. Results

The introduced methods allow us to have an in-depth look at the expansion of the wave-function $\psi(x,t)$ in position-space. In order to get a sense for the diffusion, classical comparable observables and mappings into phase-space are being observed and a frequency analysis/Fourier-transform of the wave-function is performed.

3.1. Classical Explanation for Transport: Chaotic Trajectories

3.1.1. Observing Diffusion in the Classical Model

The usual standard map can be modified to drop its restriction on the $[0, 2\pi] \times [0, 2\pi]$-cell in phase-space caused by the modulo operator. One might link a trajectory which leaves this initial cell with one contributing to quantum transport in the quantum mechanical model. For arbitrary initial coordinates within the initial cell in phase-space, statistics were made whether the trajectory sticks to the initial cell or not. The grid of these initial coordinates was choosen equidistantly.

Linking the leaving trajectories out of the initial cell to the diffusion process of $\psi(x,t)$ over time in position-space, this might be an indicator why or why not or how quickly a state expands in position-space for a given parameter set k, τ.

Figure 3.1 shows an $[1400] \times [1400]$ equidistant grid of initial conditions in the initial cell of the classical Kicked Rotor. The color of each point shows whether the trajectory leaves the initial cell after a large amount of Kicks, in this case 10000 kicks.

Obviously, trajectories starting inside of the central island in Figure 3.1 are locked to this area of phasespace and therefore are of no further interest. This leaves trajectories starting outside this stable region to be observed.

Figure 3.2 shows, how quickly the trajectories starting outside of the central island leave the initial cell.

If this amount of trajectories is interpreted as the probability of a state to stay in the initial cell, this observable could describe the likeliness of diffusion of a quantum state depending on $K = k\tau$.

A function to describe this "drop" of probability depending of the number of kicks is introduced.
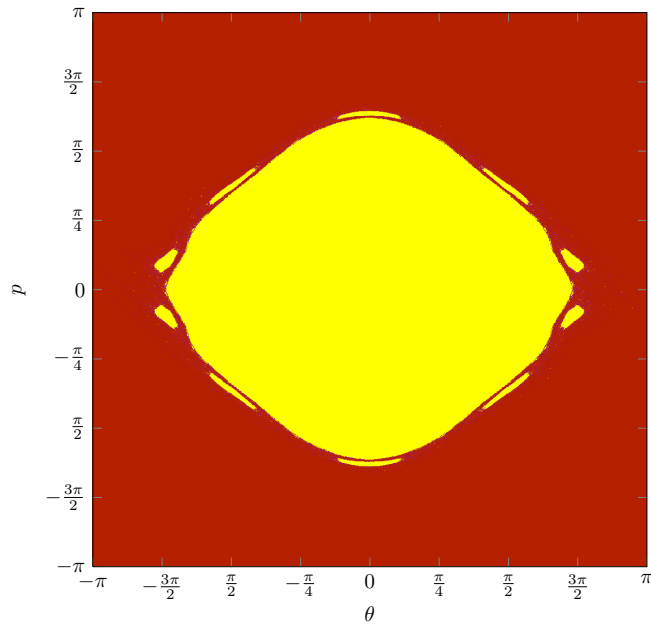
Figure 3.1.: Overview of trajectories leaving the initial cell depending on their initial conditions. The red area marks initial conditions of trajectories which leave the first, initial cell after a large number of iterations. The yellow area marks those initial conditions, whose trajectories do not leave the initial cell for a very large amount of iterations. Therefore, this area represents the regular regime of the Standard Map. The central island is clearly visible, being surrounded by a first resonance chain of order 10:1.
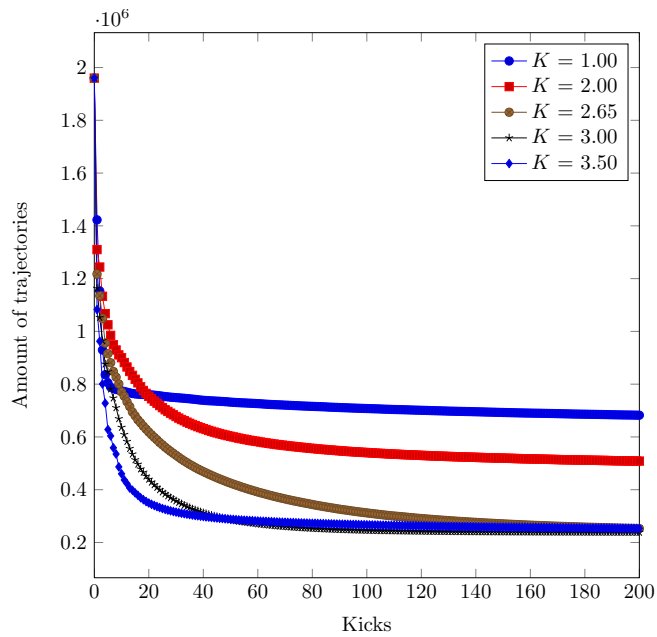

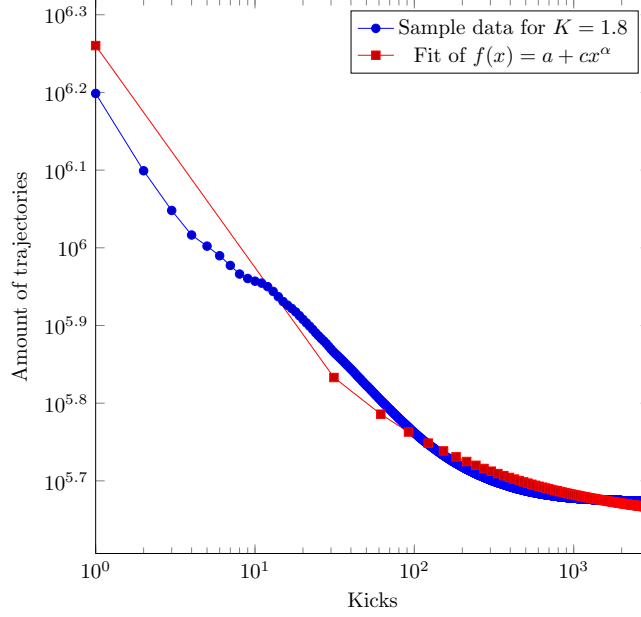Figure 3.2.: Number of trajectories in Initial Cell

Figure 3.3.: Exemplary fit of $f(x) = a + cx^\alpha$ to number of trajectories in itial cell on loglog-axis.

Then, a correlation between a certain parameter of the possible fit-function and the Survival Probality introduced in [14] is found. A parameter like a slope or decay rate of this fit-function can be interpreted as a quantum mechanical diffusion rate, which can be linked to the Survival Probability.

It can be assumed, that the curves in Figure 3.2 approximately are of the kind $f(x) = a + cx^\alpha$ (a plot with logarithmic y-axis didn't show linear behaviour, so an exponential fit wouldn't make sense). The parameter to be compared with the Survival Probability therefore is α. Even though this choice of fit-function wasn't the ultimate choice, its simplicity still enabled a comparison of one parameter (instead of maybe two or more fitting parameters defining other fitting-functions) with the Survival Probability.

Figure 3.4 contains the comparison of the the fitting parameter α and the Survival Probability depending on $K = k\tau$ for $\tau = 1$. A clear analogy of the classical decay and the quantum mechanical Survival Probability can be observed: Both curves tend to describe growing diffusion for growing K. However, extremes of both curves do not fully comply with each other. This might be explained, due to the expanded character of the quantum state, which behaves differently from what would be expected from the classical Kicked Rotor. However, both curves show a minimum for $K \approx 2.3$. This coincides with the splitting off of a resonance chain of the Standard Map and a minimum of the central regular area of the Standard Map which will be discussed later.

For higher K, both curves grow again until a maximum between $K \approx 2.4$ and $K \approx 2.8$, meaning both curves indicate a more stable or localized quantum state in position-space. In conclusion, the introduced classical decay exponent α seems to be a good indicator for the diffusion of $\psi(x, t)$ for $K \in [1, 2.8]$.
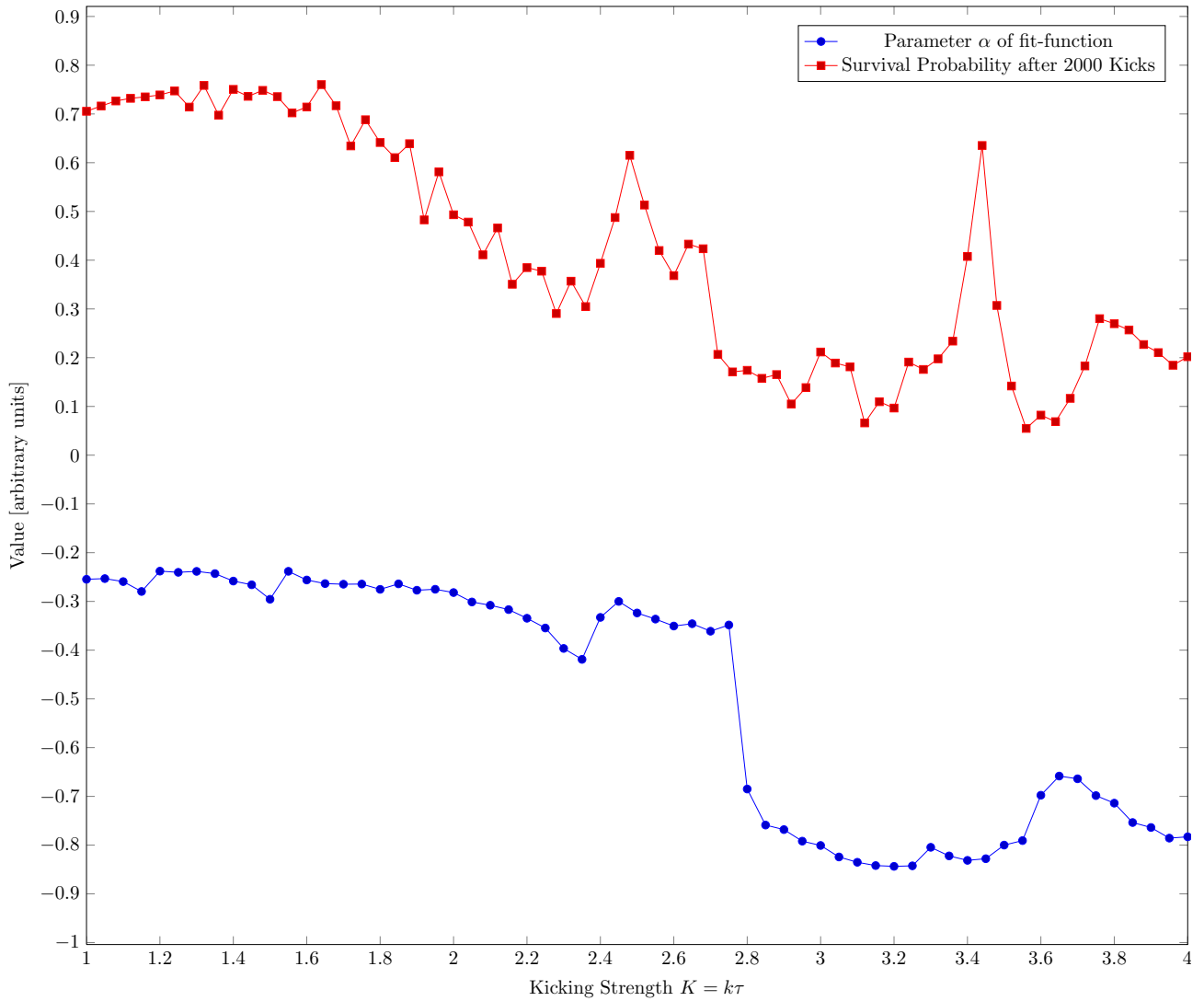
17

Figure 3.4.: Comparison of K-dependence of exponents α of fit-functions and Survival Probability. Note: A more negative expontent indicates a more instable regime or a lower Survival Probability.
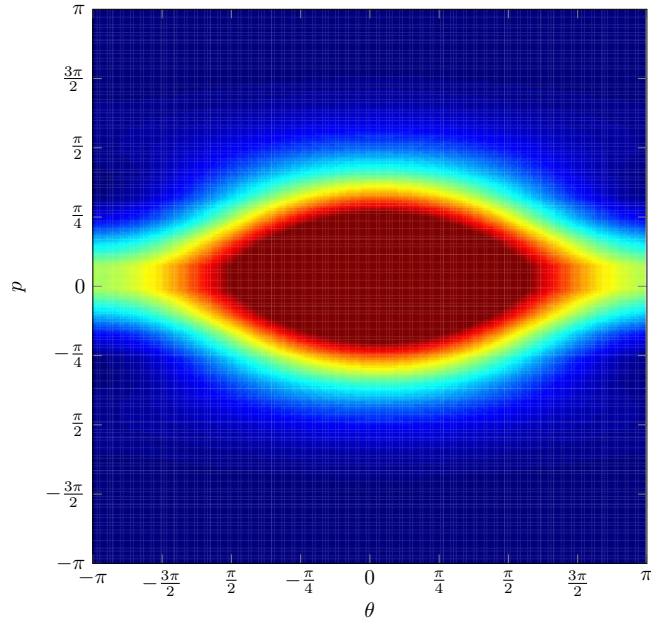
Figure 3.5.: Husimi-mapping of initial Gaussian state

3.2. Phasespace-Mappings of QKR time-evolution

The hints given in the previous chapter lead to the question how much probability of the Quantum Kicked Rotor states actually live in areas of classical chaos. This suggests the usage of Husimi-mappings: These allow to project a quantum state onto classical phase-space as it can be seen in Figure 3.5.

3.2.1. Testing the Husimi-Mapping

To provide a good understanding of the Husimi-Mapping, it was tested with the well-known coherent Gaussian state, which is used for the Quantum Kicked Rotor as initial state as well. When setting $\sigma_{theta} = 2\sigma_n$ with respect to $\sigma_\theta \sigma_n = \frac{1}{2} \Rightarrow \sigma_\theta = 1$, this state has a ratio of 2:1 for the variance in angular momentum and angle direction and therefore should transform to a circle/ellipsis stretched in momentum-direction in classical phasespace. This can be clearly seen in Figure 3.5, where the same colours show the areas of equal probability density.

3.2.2. Husimi-Mapping the Quantum Kicked Rotor time evolution

Using the Husimi-mapping for the time evolution of a Quantum Kicked Rotor, the state can be seen following an anti-clockwise "eight" as sketched in Figure 3.6. The time of a state starting in the center of the corresponding classical central island to come back to it's initial form is about 4-5 kicks. For states starting on instable fixed-points at $(0, \pi)$ this time goes up to around 40-50 kicks. These states seem to get stuck in a "transport"-area just above and below the central island area (see Figure 3.7).
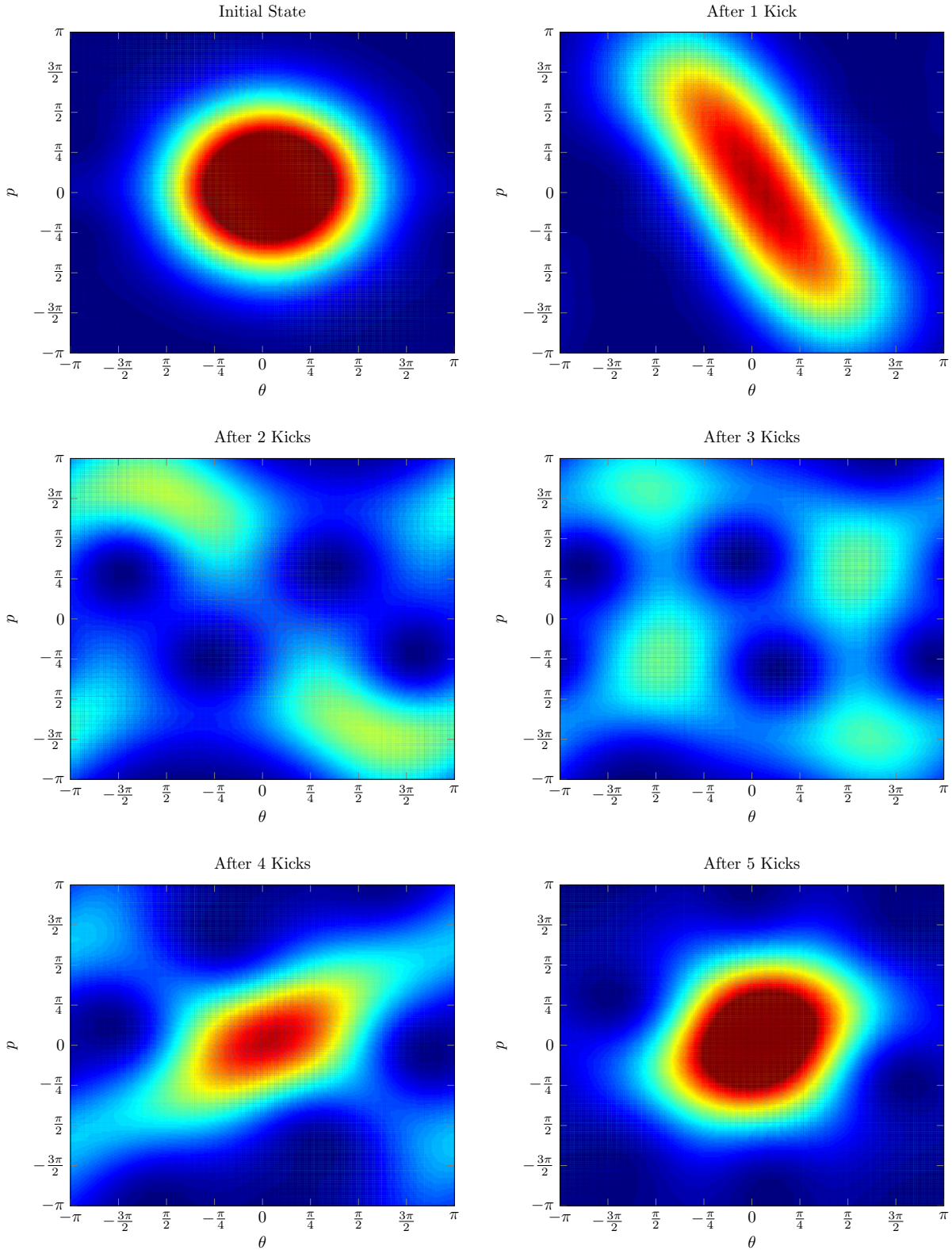
Figure 3.6.: Time evolution of Quantum Kicked Rotor mapped to classical phasespace. Note: This behaviour repeats after the timesteps shown above with a constant periodicity of around 5 kicks. The shape of the projected states stays the same. This was tested for a very larger kick number for various parameters k, τ (up to 10000 kicks).
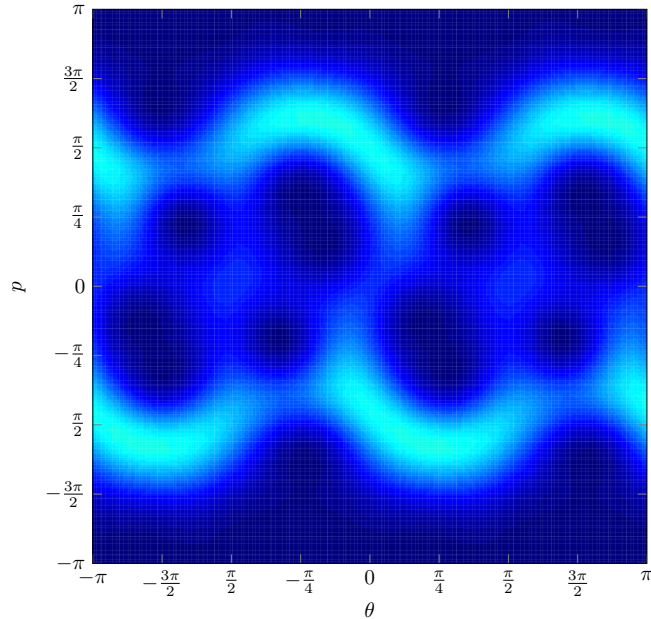
Figure 3.7.: Husimi-mapping of state stuck in "transport"-area

Due to the periodicity of the system, these states don't appear to be in movement. But in an unfolding-scenario, this transport might contribute to transport and thus diffusion of $\psi(x,t)$. States might not only come in touch with this area when starting at $(0,\pi)$, but also as β-rotors with a corresponding momentum offset β.

Figure 3.6 shows the first six kicks of the time evolution of the Quantum Kicked Rotor. Starting with the initial Gaussian state, it takes around five kicks for the state to be similar to its initial form again. It can be seen, that this "stable" state follows a tilted "eight" with its middle in the center of the central island. The overlap with the corresponding chaotic phase space after the second and third kick might explain the diffusive behaviour of the unfolded wave-function in position-space. As it can be seen in Figure 3.8, all classical trajectories which start in the chaotic regime, which is not restricted to its initial cell, diffuse. Therefore, the states residing in this chaos regime could partially explain quantum transport after leaving the regular regime of the central island.

Apparently, the observed behaviour is not the result of quantum mechanical tunneling. Such a short period time is too short, when comparing it to the order of magnitude of usual diffusion rates of quantum states. However, the observed state was projected onto the underlying basis of eigenstate and it can be clearly seen, that two eigenstates are dominating, as it can be seen in Figure 3.9: Their absolute squares sum up to nearly 1. With this result, an approximation can be made:

$$|\psi(t)\rangle \approx c_\alpha(t)\,|\psi_\alpha\rangle + c_\beta(t)\,|\psi_\beta\rangle \tag{3.1}$$

The resulting intensity, which is indirectly observed in the Husimi-mappings then is:
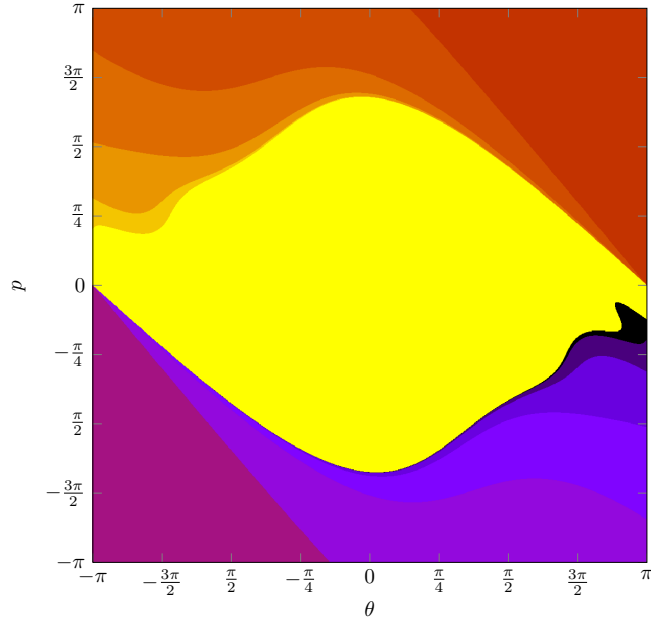
Figure 3.8.: Initial points of trajectories of the classical Standard Map are shown with colours which indicate whether they evolve to leave the initial cell on the right or left side. Yellow is for trajectories, which stay in the initial cell for at least 6 kicks (most of these stick to the central island and therefore to the initial cell for all times). Colours from red (1 kick) to light-orange (5 kicks) for the area with positive momentum determine the number of kicks needed to leave the initial cell to the right. Pink (1 kick) to purple (5 kicks) depict initial points of trajectories which leave the initial cell to the left.
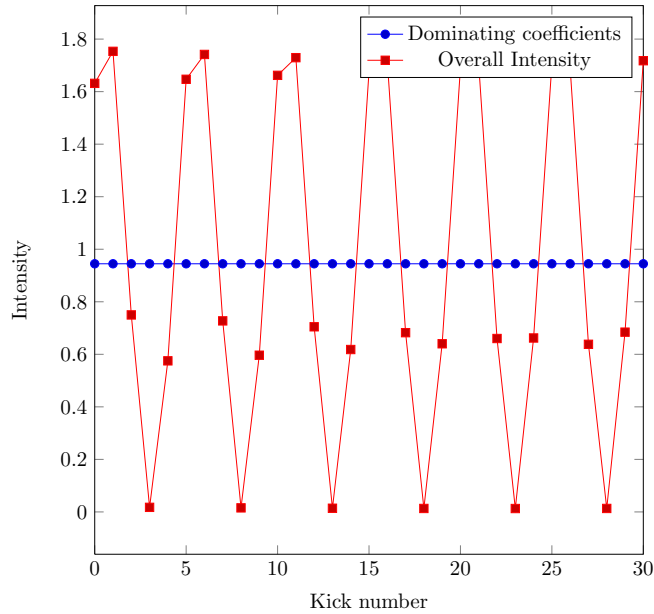

Figure 3.9.: The oscillatory intensity (approximated by equation (3.2)) comes from the phase relation of the dominant eigenstates contributing to the time evolution of the Quantum Kicked Rotor. It also explains the periocity observed in Figure 3.6.
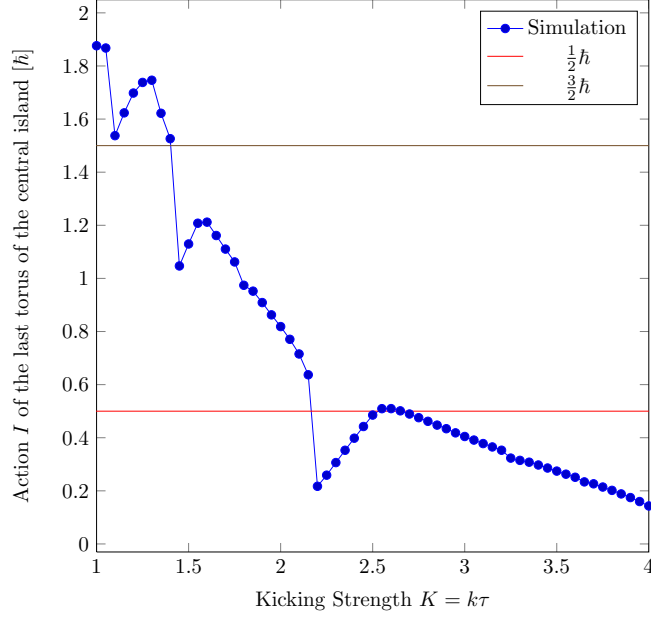
22

Figure 3.10.: The action of the outermost torus of the central island/its area show an overall decline for growing kicking strength K. Spontaneous stronger drops around $K = 1.2$, $K = 1.45$, $K = 2.15$ and $K = 3.25$ result from splitting-offs of resonance chains from the central island.

$$|\psi(t)|^2 = |c_\alpha(t)|^2 + |c_\beta(t)|^2 + 2\operatorname{Re} \tag{3.2}$$

The intensity plotted in Figure 3.9 clearly supports the periodicity statement stated from Figure 3.6. Because the magnitudes of the coefficients c_α and c_β are constant, the varying intensity is caused by the phase relation of the two dominating eigenstates.

3.2.3. Deducing information about Quantum States from the stable Area of the Standard Map

By measuring the action/area of the outermost regular torus in the central island in classical phase-space, it is possible to get a hint how many quantum states can reside on the central island. This is achieved by making the classical map symmetric, iterating from arbitrary starting points in a chaotic regime and afterwards integrating its minimal action $I(\Theta)$ over 2π. By repeating this for varying K the area of the central island can be measured for all the resulting phase space-structures.

Figure 3.10 suggests two main intervalls with different action of the central island. One lasts up to a kicking strength $K \approx 1.4$ and comes with an action above $I = \frac{3}{2}\hbar$. For a kicking strength larger than $K \approx 2.1$, the area of the central island is below $I = \frac{1}{2}\hbar$.

By considering the harmonic oscillator approximation for the regular region of the classical Kicked

Rotor [14], one can connect the known actions of the harmonic oscillator's eigenstates $I_n = \hbar(n + \frac{1}{2})$ (coming from $E_n = \hbar\omega(n + \frac{1}{2})$ and $E = I\omega$ for the harmonic oscillator, e.g. in [11] and [9]) with the measured area of the central island. In conclusion, one can state within the validity of the used approximation, that until $K \approx 1.4$ two quantum states can reside on the central island, while for $K > 2.1$ only one quantum state can do so.

This can be tested by comparing with Husimi-mappings of eigenstates of the Quantum Kicked Rotor. However, the Husimi-mappings of these eigenstates do not show the expected characteristics for the mentioned regions of $K < 1.4$ and $K > 2.1$ as clearly as expected. In both cases, there is a dominant eigenstate resembling the initial Gaussian state vaguely which one would expect as a kind of ground state. However, further eigenstates also could be counted as to be residing on the central island. Therefore, the action-interpretation stated before could not be tested.

Furthermore, the areas of the central island reflect the splitting-off of resonance chains around the central island. This can be seen for $K \approx 2.2$ and $K \approx 3.2$.

Comparing Figure 3.10 with the earlier discussed Survival Probability from Figure 3.4, one can relate an central island area below $\frac{1}{2}\hbar$ with quantum mechanical diffusion and therefore a low Survival Probablity. However, there still is a exception for $K \approx 3.4$ where the Survival Probability shows a peak. This peak was not observed in detail, since it might be caused by unwanted interference: $\psi(x, t)$ is periodic with N_β (see the Appendix: Unfolding to position-space) and therefore neighbouring wave-functions will interfere when diffusing too much. This peak-behaviour was also observed by [14].

3.3. Further Approaches to Diffusion of $\psi(x, t)$

3.3.1. Approximation of Averaged Amplitudes

To determine whether the time evolution of $\psi(x, t)$ is rather phase- or amplitude-dependend the approximation of averaged amplitudes on the level of a single Quantum Kicked Rotor with angle-representation $u_\beta(\theta)$ is introduced:

$$u_\beta(\theta_j) \equiv a_j e^{i\phi_j} \rightarrow \tilde{u}_\beta(\theta_j) = \tilde{a} e^{i\phi_j} \tag{3.3}$$

$$\tag{3.4}$$

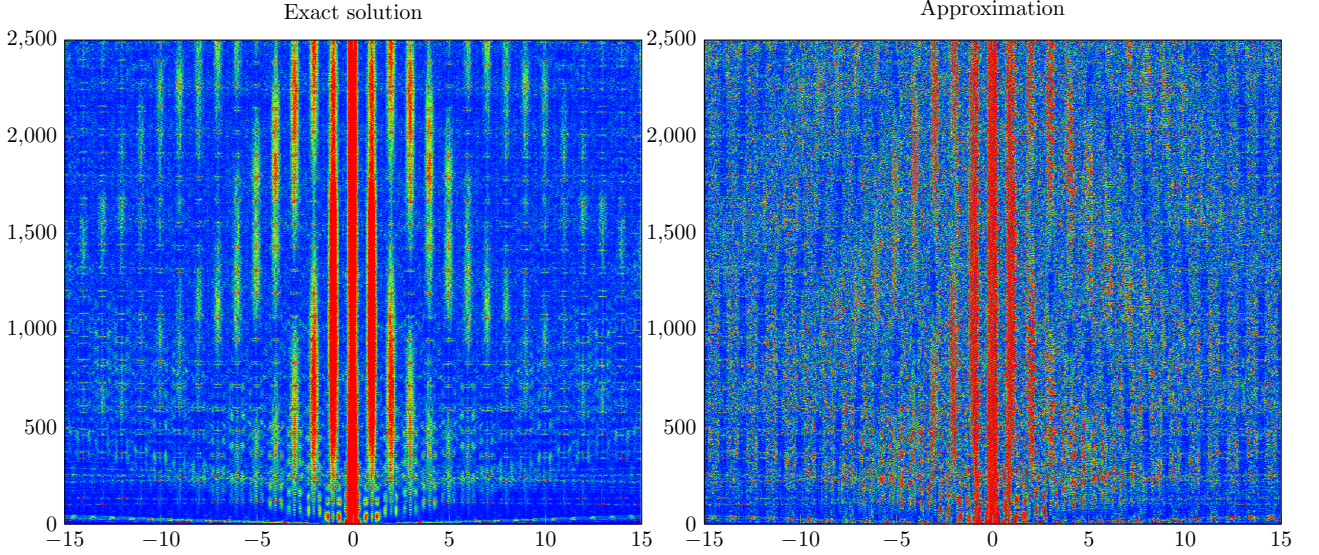where the approximation is defined by and holds:

Figure 3.11.: Diffusion of wave-function $\psi(x,t)$ in position-space over time for $K = 1.90$

$$\tilde{a} = \sqrt{\frac{1}{N_{Grid}}} \tag{3.5}$$

$$\sum_{j=1}^{N_{grid}} |\tilde{a}_\beta(\theta_j)|^2 = 1 \tag{3.6}$$

As it can be seen in Figure 3.11, the approximation keeps up with periodic interference patterns as well as a strong localization around the initial zone. This compliance was observed for all possible parameter sets of k, τ. Therefore, this problem is highly depending on the phases and much less on the amplitudes of the states.

Therefore, the time evolution of $\psi(x,t)$ is likely to depend on every contributing β-Rotor:
In the end, the vector of the sum of all state vectors with equal magnitude but different phases defines whether $\psi(x,t)$ has a maximum or a minimum. In order to distinct a subset of β-Rotors which specially cause diffusion/transport phenomena, all the others would have to add up to a vector of magnitude zero. In order to achieve this, very strict conditions on the specific phases would have to be made. This is highly unlikely, the observed phases of specific β-Rotors tend to be quite random over time. In conclusion, there are no special β-rotors contributing to the diffusion process more than others.

3.3.2. Mapping $\psi(x,t)$ to Phasespace

When mapping the wave-function in position-space to classical phasespace, one needs to modify the method introduced in the theory chapter: The underlying spaces have changed, therefore it is necessary to introduce a new coherent state in position-space which then will be used to perform the Husimi-
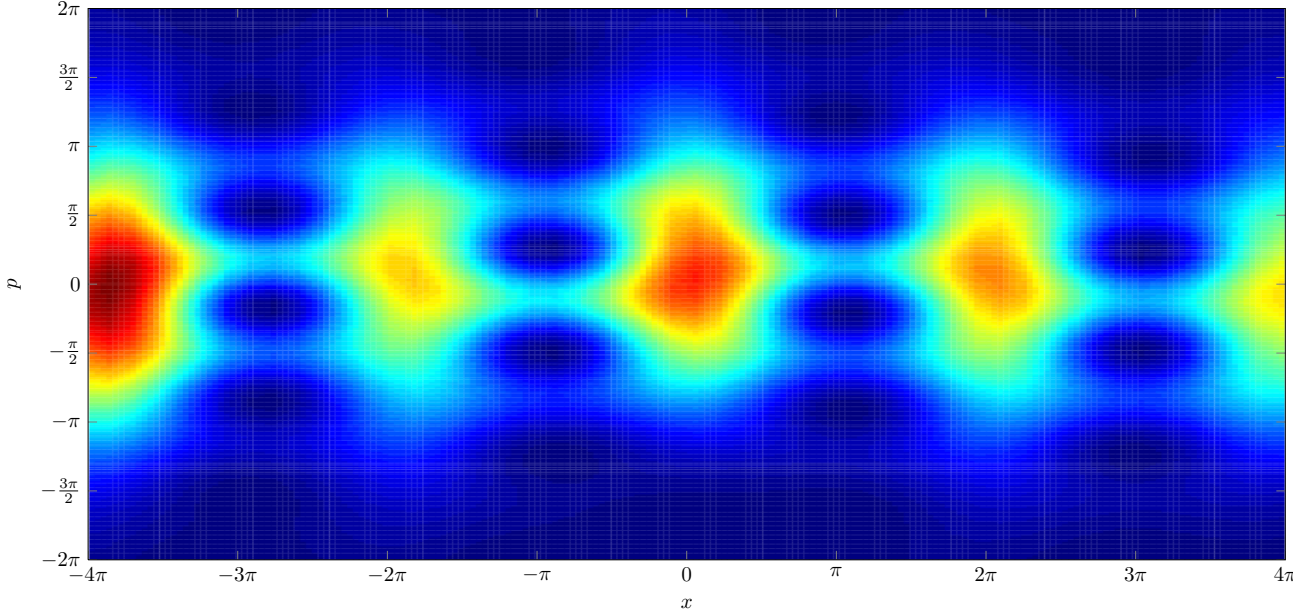
Figure 3.12.: Wave-function in position-space mapped to phasespace. The simulation resulting from parameters $k = 1.6\, \tau = 1$ qualitatively shows how the diffusion process of the unfolded Quantum Kicked Rotor at around $t = 1600$ kicks words.

mapping.

Comparison with the Husimi-mappings of a single Quantum Kicked Rotor gives further insight into the diffusion phenomenon. Starting from Figure 3.6, the expected "eight" should be seen in this mapping as well. This would explain on which path the "transport" is happening. However, when taking into account the slow diffusion processes already observed in , a diffusion process is not to be expected during the first 5 kicks.

Figure 3.12 shows a Husimi-mapping of the wave-function $\psi(x,t)$ to an extended phasespace. The "transport"-paths of the state can be observed. As suggested earlier for the Husimi-mappings of the Quantum Kicked Rotor, these follow an "eight", which is centered at $(2n\pi, 0), n \in \mathbb{Z}$ and holes around $x = (2n + 1)\pi, n \in \mathbb{Z}$ with an offset of $\frac{\pi}{4}$ or $\frac{\pi}{2}$ in momentum (which is due to the non-symmetric shape of the Quantum Kicked Rotor). The unfolded Quantum Kicked Rotor therefore has a transport mechanism comparable to the original Quantum Kicked Rotor. This observation explains the diffusion process of the unfolded Quantum Kicked Rotor qualitatively. Moreover, this transport path also parallels the classical transport trends as it was discussed with Figure 3.2.

Unfortunately, the diffusion process which can be seen easily in x-direction couldn't be directly compared with the discussed Survival Probability. While this configuration ($k = 1.6, \tau = 1$) of Figure 3.12 usually shows a higher Survival Probability and therefore less diffusion, this behaviour can't be observed for less stable configurations. A configuration with e.g. k = 2.25, $\tau = 1$ (where Survival Probability has a local minimum) didn't show as strong diffusion as the chosen configuration.
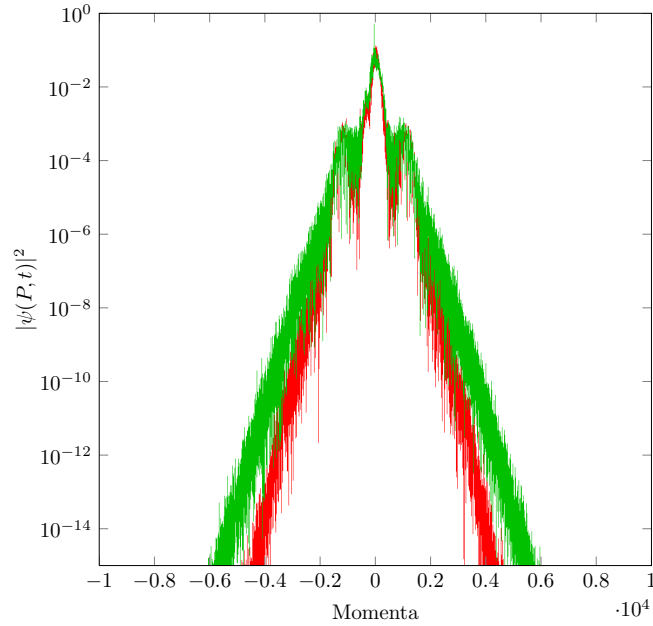
Figure 3.13.: Wave-function in position-space transformed to Momentum-Space. The chosen curves result from the parameters $k = 1.6\,\tau = 1$, where the Survival Probability at $t = 2500$ shows a minimum and $k = 2.25\,\tau = 1$, where the Survival Probability shows a maximum.

3.3.3. Analysing Peaks of $\psi(P, t)$

Performing a Fourier transform of $\psi(x, t)$ gives $\psi(P, t)$ which might offer valuable clues about the momentum components. Unfortunately, all these transforms to $\psi(P, t)$ show a localized probability density around zero momentum in P-space, as it can be seen in Figure 3.13. No specific momentum components besides the 0-momentum component and its closest neighbors dominate. This was observed for all sets of k, τ, t.

4. Conclusion

The main goal of this thesis was to extend the parameter range of the kicking strength k for which the diffusion properties of the unfolded Quantum Kicked Rotor are understood.

The analogies between the classical Kicked Rotor/Standard Map and its quantum mechanical counterpart were demonstrated. It was observed, that an ensemble of chaotic Kicked Rotor-trajectories is a reasonable approximation for the diffusive behaviour of an atom in a time- and space-periodic kicking potential. Relations between these two models were thorougly investigated by using Husimi-mappings. These allowed to gain new insights on the time evolution of the Quantum Kicked Rotor: This gave on the one hand hints about dominating eigenstates of the system with an oscillating phase relation among these eigenstates and on the other hand, first hints about the transport paths of quantum states of the unfolded Quantum Kicked Rotor were found.

Moreover, the Husimi-mapping allowed rejecting the use of the area of the central island of the Standard Map as an indicator for quantum mechanical behaviour. A direct correlation, like the number of eigenstates residing on a classical stable regime, when comparing eigenstates of the Quantum Kicked Rotor with the central island and its area was not found.

Further approaches like approximating the time evolution of the unfolded Quantum Kicked Rotor with average amplitudes of the contributing wave-functions supported that the problem heavily depends on the phase relations of the states. After introducing the Husimi-mapping for the single Quantum Kicked Rotor it was a matter of course to apply it to the unfolded version as well: This supported the theory, that a single Quantum Kicked Rotor hints at the quantum transport paths of the quantum state. Lastly, analysing the momentum-distribution of the unfolded wave-function $\psi(x, t)$ didn't return any further information.

With this thesis, the transport behavior of states of the unfolded Quantum Kicked Rotor is understood qualitatively. The analogy of the Survival Probability to the chaotic trajectories of the classical Kicked Rotor provides a hint at quantitatively explaining diffusion velocity of quantum states. It remains to clarify, which mechanism enables the quantum state to cross the classical barrier of the central island.

Future observations could focus on the area overlap of the Quantum Kicked Rotor states with regions of classical chaos. The measurements of the area of the central island could be of further use in this case. Possibly, a criterion based on area overlaps (weighted with the probability-density of the quantum state) could explain the diffusion rate of a quantum state from the stable regime of the central island into chaos. Connecting this with the qualitatively understood transport paths and first

hints at quantitative approximation of transport velocities could explain the diffusive characteristics of wave-functions of the unfolded Quantum Kicked Rotor entirely.

Bibliography

[1]   M. Abb. "Fidelity for kicked atoms at nearly resonant driving". Diploma thesis. University of Heidelberg, 2009.

[2]   S. Fishman, I. Guarneri, and L. Rebuzzini. "A theory for quantum accelerator modes in atom optics". In: *Journal of statistical physics* 110.3 (2003), pp. 911–943.

[3]   K. Husimi. "Some formal properties of the density matrix". In: *Proc. Phys.-Math. Soc. Japan.* Vol. 22. 1940, pp. 264–314.

[4]   B. Probst. "The Pendulum Approximation for Fidelity in Quantum Kicked Rotor Systems". Diploma thesis. University of Heidelberg, 2010. MA thesis.

[5]   M.G. Raizen et al. "Dynamical localization of ultracold sodium atoms". In: *Physical Review E* 60.4 (1999), pp. 3881–3895.

[6]   J.J. Sakurai, S. Tuan, and E. D. Commins. "Modern quantum mechanics". In: *American Journal of Physics* 63 (1995), p. 93.

[7]   P. Schlagheck and U. Peschel. Private communication.

[8]   K. Srihari and P. Schlagheck. *Dynamical tunneling: theory and experiment.* CRC, 2010.

[9]   T. Weigand. "Kursvorlesung PTP4: Theoretische Quantenmechanik". Lecture notes. 2011.

[10] S. Wimberger. "Chaos and Localisation: Quantum Transport in Periodically Driven Atomic Systems". PhD thesis. Ludwig-Maximilians-University Munich and Università dell' Insubri Como, 2004.

[11] S. Wimberger. "Nonlinear Dynamics and Quantum Chaos". Lecture notes. 2012.

[12] S. Wimberger, I. Guarneri, and S. Fishman. "Quantum resonances and decoherence for δ-kicked atoms". In: *Nonlinearity* 16.4 (2003), p. 1381.

[13] S. Wimberger and M. Sadgrove. "The role of quasi-momentum in the resonant dynamics of the atom-optics kicked rotor". In: *Journal of Physics A: Mathematical and General* 38.49 (2005), p. 10549.

[14] F. Ziegler. "Kicked-rotor dynamics in optical fibers". Bachelor thesis. University of Heidelberg, 2012.

A. Measuring Action

In order to estimate the action of a given torus of the classical Kicked Rotor, one would have to measure the area of the phasespace enclosed by this torus. This can be done a lot easier by using action angle-coordinates of the harmonic oscillator.. The measurement of a surface in phasespace then turns into averaging the action under variation of $\Theta \in [0, 2\pi]$.

In order to smooth the action $I(\Theta)$, the symmetric version of the classical Kicked Rotor is used:

$$q' = q + \frac{p}{2} \tag{A.1}$$

$$p' = p - K\sin(q) \tag{A.2}$$

$$q'' = q + \frac{p}{2} \tag{A.3}$$

This makes to numerical integration of $I(\Theta)$ a lot more stable.

The integration itself is performed by starting trajectories in the seemingly chaotic regime close to the central island in the Kicked Rotor phasespace. Starting from there, the trajectories are observed for a large number of iterations [7].

These trajectories then can be observed in action angle-space. The area below the torus with minimal Action has to be found by numerical integration in order to average the action in the given intervall and thus obtaining the action of the central and stable island of the Standard Map in phasespace.

It is necessary to find the lowest curve in this picture which represents a stable torus. Since the numerical integration happens in a discrete grid of finite bin-width, one can easily pick for the action the data-point with the lowest action in the respective bin. If there is no such data-point or the deviation from neighbouring data-points on the designated curve is too high, one has to interpolate a data-point. This was done by linear interpolation, which is good enough, given the accepted range of error for the results. However, for a large enough number of iterations (around 10^{10}), this interpolating routine wasn't necessary anymore.

B. Unfolding to Position-space

The unfolding of the initial N_β β-Rotors to position-space was introduced as

$$\psi(x,t) = \int_0^1 e^{i\beta x}\psi_\beta(x=\theta,t)d\beta \tag{B.1}$$

The resulting wave-function shows a periodicity in x of periodicity N_β. Therefore it can be normalized to 1 over one period, which is the area $x \in [-\frac{N_\beta}{2}, \frac{N_\beta}{2}]$. Since the numerics underlying this thesis were performed in C and no usage of a custom complex data-structure was made, this calculation was implemented in the following way.

$\psi_\beta = \psi_\beta(x=\theta,t)$ denotes a wave-function residing on the Rotor in angle-space, $\psi = \psi(x,t)$ denotes the unfolded wave-function in position-space. At position x in position-space, ψ_β will be evaluated at $\theta = x \mod 2\pi$.

Introducing

$$\psi_\beta^r := \operatorname{Re}\psi_\beta \tag{B.2}$$

$$\psi_\beta^i := \operatorname{Im}\psi_\beta \tag{B.3}$$

ψ (B.1) can be expanded into:

$$\psi = \int_0^1 (\cos(\beta x) + i\sin(\beta x))(\psi_\beta^r + i\psi_\beta^i)d\beta \tag{B.4}$$

For numerical realisation ψ will also be splitted into its real ψ^r and imaginary part ψ^i:

$$\psi^r = \int_0^1 \cos(\beta x)\psi_\beta^r - \sin(\beta x)\psi_\beta^i d\beta \tag{B.5}$$

$$\psi^i = \int_0^1 \sin(\beta x)\psi_\beta^r + \cos(\beta x)\psi_\beta^i d\beta \tag{B.6}$$

For numerical realization the problem has to be discretized.

$$\int_0^1 d\beta \rightarrow \sum_{i=0}^{N_\beta-1} \Delta\beta \tag{B.7}$$

$$\Delta\beta = \frac{1}{N_\beta} \tag{B.8}$$

With introducing the β-grid of constant distance and weight, the weight-function $\rho(\beta) = \sum_{j=0}^{N_\beta-1} \delta(\beta - \frac{j}{N\beta})$ was assumed. This reflects an equally weighted superposition of all N_β Quantum Kicked Rotors yielding a wave-function in position-space launching from one centered initial zone.

This yields, ready for straight-forward implementation:

$$\psi^r = \frac{1}{N_\beta} \sum_{j=0}^{N_\beta-1} \cos(\beta x)\psi_\beta^r - \sin(\beta x)\psi_\beta^i \tag{B.9}$$

$$\psi^i = \frac{1}{N_\beta} \sum_{j=0}^{N_\beta-1} \sin(\beta x)\psi_\beta^r + \cos(\beta x)\psi_\beta^i \tag{B.10}$$

Since x usually is a multiple of 2π, the possible values of βx should be pre-computed for all occuring tupels (β, x) in a lookup-table. Moreover, one can make use of scalar-product implementations for the four expressions like $\cos(\beta x)\psi_\beta^r$: First calculate the two factors and store them into an array, then implement it like a scalar-product $\langle a, b \rangle$. Since many modern CPUs have high-speed implementations of the scalar-product on low-level, this method is significantly faster then doing a for-loop as suggested by the summation in (B.9) and (B.10). However, this might not apply, if this kind of optimization is already done by a framework. That might be the case if using a script-language + some math-framework which is linking to a low-level-library.

The following code performs the lookup-table for the trigonometric calculations.

```
typedef struct {
  int a;
  int b;
  double* data;
} Int2d;

Int2d args_unfold_values = {Nbeta,Nposition};
```

```
Int2d cos_unfold_values = {Nbeta,Nposition};
Int2d sin_unfold_values = {Nbeta,Nposition};


args_unfold_values.data = malloc(args_unfold_values.a *
        args_unfold_values.b * sizeof *args_unfold_values.data);
cos_unfold_values.data = malloc(cos_unfold_values.a *
        cos_unfold_values.b * sizeof *cos_unfold_values.data);
sin_unfold_values.data = malloc(sin_unfold_values.a *
        sin_unfold_values.b * sizeof *sin_unfold_values.data);



for (int beta_index_unfolding = 0; beta_index_unfolding < Nbeta;
  ++beta_index_unfolding)
{
  for (int position_index = 0; position_index < Nposition; ++position_index)
  {
        //Now arr2d[r][c] (the usual way) translates into
          arr2d.data[r * arr2d.b + c]

        args_unfold_values.data[beta_index_unfolding *
          args_unfold_values.b + position_index]
          = beta[beta_index_unfolding]*position[position_index];
  }
}

int Nunfoldargs = Nposition*Nbeta;

vvsincos(sin_unfold_values.data,cos_unfold_values.data,
  args_unfold_values.data,&Nunfoldargs);
```

The following code performs the unfolding of the β-rotors $\psi(\theta, t)$ to obtain $\psi(x, t)$. The rotors are saved with respect to their specific β and angle discretization in the array "out_array".

```
for (int position_index = 0; position_index < Nposition; ++position_index)
  {
  angular_index = (position_index + Nmitte) % Nmomentum;

  real1 = 0;
  real2 = 0;
  imag1 = 0;
  imag2 = 0;
```

```
for (int beta_index_unfolding = 0; beta_index_unfolding < Nbeta;
      ++beta_index_unfolding)
{
      cos_value = cos_unfold_values.data[beta_index_unfolding
        * cos_unfold_values.b + position_index];
      sin_value = sin_unfold_values.data[beta_index_unfolding
        * sin_unfold_values.b + position_index];

      out_real = out_array[beta_index_unfolding][angular_index][0];
      out_imag = out_array[beta_index_unfolding][angular_index][1];

      real1 = real1 + cos_value*out_real;
      real2 = real2 - sin_value*out_imag;
      imag1 = imag1 + cos_value*out_imag;
      imag2 = imag2 + sin_value*out_real;
}

real = (real1+real2)*beta_grid;
imag = (imag1+imag2)*beta_grid;

position_space[kick_index][position_index] = real*real+imag*imag;
}
```

C. Validity of quantum mechanical Simulations

Since this thesis develops the diffusion theory developed in [14] further the numerical realisation of the Quantum Kicked Rotor was compared for a common situation. In figure Figure C.1 compliance of the both implementations in Fortran [14] or C (this thesis) can be clearly seen.

The small visible error is explained by a differing normalization method used by Ziegler. It depended on more parameters than the periodicity of the wave-function in position-space, which is used in this thesis.
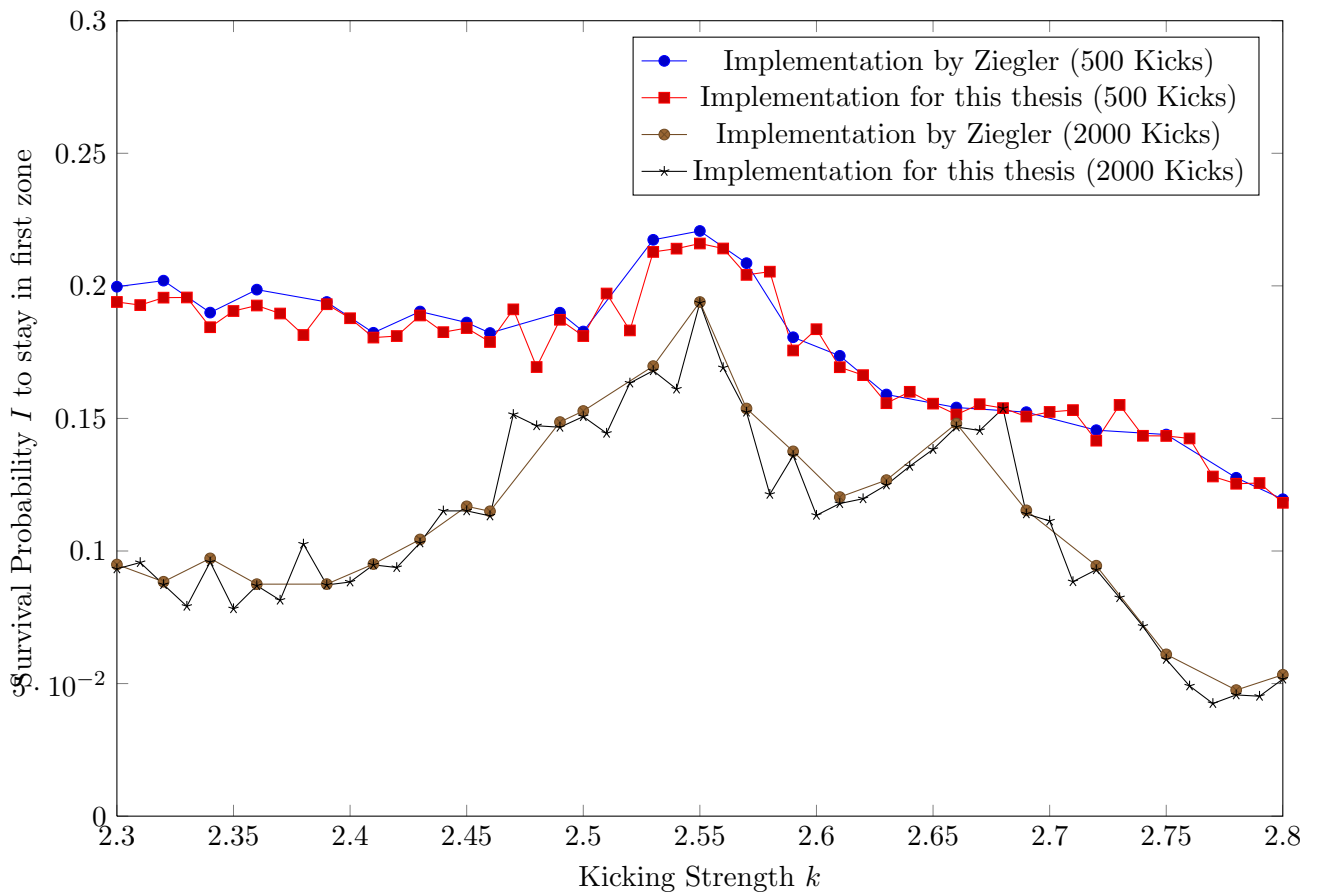
Figure C.1.: Comparison of different implementations of the unfolded Quantum Kicked Rotor

Erklärung

Ich versichere, dass ich diese Arbeit selbstständig verfasst und keine anderen als die angegebenen Quellen und Hilfsmittel benutzt habe.

Heidelberg, den ...,